*Int. J. Electrochem. Sci.*, 14 **(2019)** 634 – 650, doi: 10.20964/2019.01.57

International Journal of
ELECTROCHEMICAL
SCIENCE
www.electrochemsci.org

# $CO_2$ Capture Process and Corrosion of Carbon Steel in [Bmim][Lys]-$K_2CO_3$ Aqueous Solutions

*Jialin Xie, Li Zhang, Dong Fu*[*]*,Hongtao Zhu*

School of Environmental Science and Engineering, North China Electric Power University, Baoding, 071003, China
[*]E-mail: fudong@tsinghua.org.cn

*Received:* 3 October 2018/ *Accepted:* 6 November 2018 / *Published:* 30 November 2018

The corrosion of carbon steel in carbonated 1-butyl-3-methylimidazolium lysinate ([Bmim][Lys])-potassium carbonate ($K_2CO_3$) aqueous solution was investigated by using a CHI602E electrochemical analyser. The time-dependent absorption capacity, polarization behaviour and corrosion rate of carbon steel in carbon dioxide ($CO_2$)-loaded $K_2CO_3$ aqueous solution and [Bmim][Lys]-$K_2CO_3$ aqueous solution were measured. The effects of temperature, the mass fraction of [Bmim][Lys]/$K_2CO_3$ and $CO_2$ loading on the corrosion rate were demonstrated. The pH values of $CO_2$-loaded $K_2CO_3$-[Bmim][Lys] aqueous solutions were measured, and the variations in $H^+$ concentration and the effect of $H^+$ concentration on the corrosion rate were analysed. Our experiments showed that when activated by [Bmim][Lys], $K_2CO_3$ aqueous solution demonstrated a higher $CO_2$ absorption capacity, higher $CO_2$ absorption rate and lower corrosion rate for carbon steel. Compared with the commercially applied diethanolamine (DEA, 3%) - $K_2CO_3$ (25%) aqueous solution, the [Bmim][Lys] (7.5%)-activated $K_2CO_3$ (25%) aqueous solution can not only achieve a higher $CO_2$ absorption capacity, lower the corrosion of carbon steel and achieve a similar $CO_2$ absorption rate but also decrease the energy cost due to its advantages of higher concentration and lower water content; thus, the investigated solution has very good application potential in the $CO_2$ capture process.

**Keywords:** $K_2CO_3$, [Bmim][Lys], $CO_2$, absorption, corrosion.

## 1. INTRODUCTION

In recent decades, the reduction of carbon dioxide ($CO_2$) emissions has attracted increasing attention around the world [1,2], and many technologies [3-7] have been proposed for separating $CO_2$ from various gas streams. Among the currently available technologies, chemical absorption is considered one of the most effective approaches due to its satisfactory $CO_2$ removal efficiency and absorbent regeneration efficiency [8].

As a typical representative of chemical absorption, potassium carbonate ($K_2CO_3$)-based absorption technology has been commercially used for many years [9,10] because it has the advantages of low cost, low toxicity, low heat of absorption, low solution loss, no formation of heat-stable salts and no thermal and oxidative degradation [10]. However, the $K_2CO_3$-based absorption process also has drawbacks such as a slow absorption rate, leading to poor $CO_2$ mass transfer [11-15]. Since the post-combustion $CO_2$ absorption process must operate under flue gas conditions, such as a relatively low temperature and atmospheric pressure, enhancing the absorption rate is necessary. In addition to the poor $CO_2$ mass transfer, the serious corrosion of carbon steel is another drawback in the $K_2CO_3$-based absorption process and may severely damage the equipment, such as absorbers, pipelines and valves, and result in a reduction in the process efficiency and increase in maintenance costs.

To minimize the corrosion of carbon steel, many researchers have focused on the control of $K_2CO_3$ concentration, operating temperature and $CO_2$ loading; however, a decrease in $K_2CO_3$ concentration and $CO_2$ loading may lower the absorption capacity and increase the energy cost. The development of a new absorbent that can simultaneously achieve a higher $CO_2$ absorption capacity and higher $CO_2$ absorption rate yet lower the corrosion rate of carbon steel is of great significance for improving $K_2CO_3$-based absorption technology.

Previous studies have shown that many activators such as amines [16-21] and amino acids [22-26] can significantly enhance the $CO_2$ absorption in $K_2CO_3$ aqueous solutions. In addition to amines and amino acids, ionic liquids (ILs) are considered to be potential activators for facilitating the rate of absorption. As new promising solvents for $CO_2$ capture, ILs have numerous advantages, such as non-volatility, a low melting point, ease of recycling, high thermal stability and adjustable physicochemical structures [27-29]. In recent decades, ILs have attracted increasing attention in the $CO_2$ capture process. Hu [30] investigated the $CO_2$ absorption performance of five synthesized amino ILs, and the results showed that ILs with more amino groups have a higher $CO_2$ absorption capacity. Wappel [31] measured the viscosities and $CO_2$ absorption kinetics of a series of ILs and blends of ILs and compared the results with reference data for 30 wt% $K_2CO_3$ aqueous solution. The results showed that the viscosities of all diluted ILs and selected IL blends were larger than those of the $K_2CO_3$ aqueous solutions and that the $CO_2$ absorption kinetics of the ILs and IL blends were much faster than those of the $K_2CO_3$ aqueous solutions. Moreover, metals and alloys have a very low corrosion tendency in aggressive solution when ILs containing imidazole and its derivatives are added because the lone electron pairs in nitrogen atoms are likely to promote the adsorption of compounds on metallic surfaces [32-34]. Recently, Zhang [35,36] and Ashassi-Sorkhabi [37] evaluated the corrosion of mild steel in acidic solution containing alkyl-imidazolium ILs. Their results showed that the mild steel exhibited very low corrosion performance. Zheng [38] investigated the corrosion behaviour of mild steel in sulfuric acid solution containing two imidazolium-based ILs (1-octyl-3-methylimidazolium bromide ([OMIM]Br) and 1-allyl-3-octylimidazolium bromide ([AOIM]Br)). Their results showed that the mild steel exhibited a lower corrosion performance in sulfuric acid containing [AOIM]Br than in sulfuric acid containing [OMIM]Br. Therefore, ILs containing imidazolium should cause little corrosion to mild steel equipment when absorbing $CO_2$. In addition, ILs with anionic amino acids are considered good $CO_2$ absorbents because they can achieve equimolar $CO_2$ absorption and take advantage of their negligible vapor pressure and remarkable thermal stability [39-41]. Among ILs, amino-acid ionic liquids (AAILs) are very attractive

because they have large $CO_2$ solubility and can facilitate $CO_2$ absorption in aqueous solutions of amines [42-47]; in particular, 1-butyl-3-methylimidazolium lysinate ([Bmim][Lys]) has very strong affinity to $CO_2$ because there are two primary amine functional groups present in basic and polar side chains on its molecular structure [48,49]. Fu [42] showed that when activated by very small amount of [Bmim][Lys], MDEA-[Bmim][Lys] aqueous solution can absorb $CO_2$ with a high rate and high capacity.

According to the aforementioned advantages, it is reasonable to expect that both the $CO_2$ absorption performance and corrosion of carbon steel can be considerably improved in $K_2CO_3$-[Bmim][Lys] aqueous solution. However, studies concerning the $CO_2$ absorption capacity and corrosion behaviour of carbon steel in $CO_2$-[Bmim][Lys]-$K_2CO_3$ aqueous solution have rarely been reported to date. The main purpose of this work is to simultaneously achieve a higher $CO_2$ absorption capacity, higher $CO_2$ absorption rate and lower corrosion to carbon steel by using [Bmim][Lys]-activated $K_2CO_3$ aqueous solutions. To this end, (1) the time-dependent $CO_2$ absorption capacity and absorption rate were measured; (2) the polarization behaviour and corrosion rates of carbon steel in $CO_2$-$K_2CO_3$ aqueous solutions and $CO_2$-[Bmim][Lys]-$K_2CO_3$ aqueous solutions were measured; (3) the pH values of $CO_2$-loaded $K_2CO_3$-[Bmim][Lys] aqueous solutions were measured, and the variation in $H^+$ concentration and the effect of $H^+$ concentration on corrosion rate were analysed; and (4) the effects of solution concentration, temperature and $CO_2$ loading on corrosion rate were demonstrated.

## 2. EXPERIMENTAL

### *2.1 Solutions and materials*

The samples used in the absorption experiments are presented in Table 1. They were used without further purification. An analytical balance (Jingtian FA1604A) with an accuracy of 0.1 mg was used to weigh all required chemicals. The water contents (in mass percent) of $K_2CO_3$ and [Bmim][Lys] were respectively 0.22% and 0.21% (determined by using the Karl Fischer method, as stated by the supplier), and this content were accounted for upon solution preparation. $K_2CO_3$ and $K_2CO_3$-[Bmim][Lys] aqueous solutions were prepared by adding deionized water (electrical resistivity >15 MΩ·cm at 298 K) obtained from a Heal Force ROE (reverse osmosis electrodeionization)-100 apparatus to weighed quantities of $K_2CO_3$ and [Bmim][Lys]. Taking the purities and water contents into account, the uncertainties of the mass fraction of $K_2CO_3$ and [Bmim][Lys] were estimated to be $u(w) = \pm 0.005$.

The specimens for corrosion tests were made of carbon steel (AISI 1020) in this work. The chemical composition (in mass percent, %) was 0.20 C, 0.25 Si, 0.50 Mn, 0.03 P, 0.03 S and Fe (balance). The specimens (10 mm×10 mm×3 mm) were ground, polished and then sealed with resin with an exposed area of 10 mm×10 mm. The specimens were connected with copper wires to make the working electrodes for the electrochemical tests.

**Table 1.** Sample description.

| Chemical name | CAS | Purity (mole fraction, as stated by the supplier) | Water content (mass percent, as stated by the supplier) | Source |
|---|---|---|---|---|
| $K_2CO_3$ | 584-08-7 | $x \geqslant 0.99$ | 0.22% | Fuchen Chemical Reagent |
| [Bmim][Lys] | 1084610-48-9 | $x \geqslant 0.99$ | 0.21% | Chengjie Chemical Reagent |
| carbon dioxide | 124-38-9 | $x \geqslant 0.9999$ | | Hanjiangxue Gas |
| water | 7732-18-5 | Electrical resistivity > 15 MΩ cm at $T$ = 298 K | | Heal force ROE-100 apparatus |

*2.2 Apparatus and procedure*

The experimental system for absorption is shown in Fig. 1, with all the various parts of the apparatus and the measuring devices included. During absorption, $CO_2$ from a high-pressure tank (concentration $C_0 \geqslant 0.9999$) passed through the mass flow controller to maintain a constant flow rate of $v_{CO2}$=200 ml/min, then flowed into the absorption bottle and was absorbed by the solution. The residual and unabsorbed gas first flowed into the desiccator, then into the $CO_2$ analyser and finally into the mass flow metre (MFM). The $CO_2$ concentration ($C_i$) was measured by the $CO_2$ analyser, and the flow rate ($v_i$) was measured by the MFM. $C_i$, $v_i$ and the corresponding time $t_i$ were simultaneously recorded by the computer (interval time $\Delta t$ =1 s). The absorption was terminated when there was almost no change in $v_i$ for 100 s. The mass of absorbed $CO_2$ was calculated from $273.15\times44/22.4\times[0.9999v_{CO2}t/T_0-\Sigma v_iC_i\Delta t/T_1]$, in which $t$ is the total absorption time, and $T_0$ and $T_1$ are the temperatures of $CO_2$ flowing out of the mass flow controller (MFC) and desiccator, respectively. After the mass of absorbed $CO_2$ was obtained, the $CO_2$ loading ($\alpha$) was calculated from $\alpha=n_{CO2}/(n_{K2CO3}+ n_{[Bmim][Lys]})$, in which $n_{CO2}$ is the moles of loaded $CO_2$, and $n_{K2CO3}$ and $n_{[Bmim][Lys]}$ are the moles of $K_2CO_3$ and [Bmim][Lys], respectively, in the unloaded aqueous solution. Carbonated aqueous solutions with different $CO_2$ loadings were prepared according to the methods mentioned in the work of Weiland [50], Amundsen [51] and Fu [42,44,52]; once the carbonated solution had been prepared using the equipment shown in Fig. 1, varying proportions of unloaded and loaded solutions were mixed together to produce a set of samples.

The experimental system for corrosion testing was composed of one electrochemical workstation (CHI602E, manufactured by Shanghai Chenhua instrument Co., Ltd.), one thermostat water bath, one corrosion cell and one data recorder. Within 1 hour prior to the electrochemical tests, the specimens were mechanically polished with 600, 1000 and 1500-grit silicon carbide metallurgical papers, degreased with methanol, dried with hot air and stored in a dry cabinet. Electrochemical tests were then carried out in a 500 ml corrosion cell immersed in a thermostatic bath. The temperature ranged from 303.2 K to 323.2 K. A three-electrode electrochemical cell was used (working, reference and counter electrode). The carbon steel was used as the working electrode. A Pt electrode was employed as the counter electrode, and a $Hg/HgCl_2$ electrode was employed as the reference electrode. Once the open circuit potential

(OCP) of the cell was stable (OCP<1 mV/min), the polarization curves were measured by the CHI602E with a computer recording the data (potential range: -200 mV to +200 mV vs. OCP, scan rate: 0.0002 V/s).

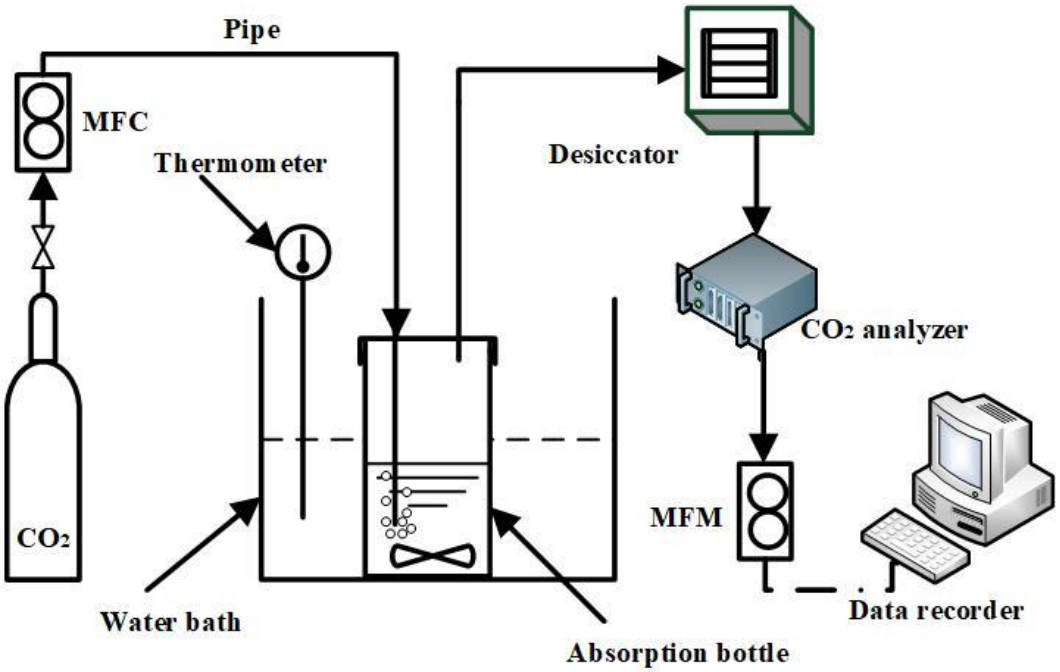


**Figure 1.** Schematic diagram of absorption.

## 3. RESULTS AND DISCUSSION

### *3.1 $CO_2$ absorption performance*

The absorption performances of $CO_2$ in [Bmim][Lys]-activated $K_2CO_3$ and diethanolamine (DEA)-activated $K_2CO_3$ aqueous solution were measured at 313.2 K. The mass fraction of $K_2CO_3$ ($w_{K2CO3}$) was 0.25. The mass fractions of [Bmim][Lys] ($w_{[Bmim][Lys]}$) and DEA ($w_{DEA}$) were 0.075 and 0.03, respectively. Moreover, the absorption performance and capacity of $CO_2$ in $K_2CO_3$ aqueous solution at 313.2 K and $w_{K2CO3}$=0.75 were taken directly from our previous work [53]. The time-dependent $CO_2$ absorption capacities are shown in Fig. 2. One finds from the plot that without [Bmim][Lys], $CO_2$ was absorbed slowly in $K_2CO_3$ aqueous solution. When a small amount of [Bmim][Lys] was added to the $K_2CO_3$ aqueous solution, the absorption time corresponding to saturation decreased significantly, and the amount of absorbed $CO_2$ increased substantially. In particular, the mass of absorbed $CO_2$ changed from 6.46 g $CO_2$/100 g aqueous solution to 7.53 g $CO_2$/100 g aqueous solution, which indicates that [Bmim][Lys] can not only be used as an accelerator but also absorb a certain amount of $CO_2$. Compared with [Bmim][Lys] (7.5%), DEA (3%) also accelerated the absorption of $CO_2$, but the mass of absorbed $CO_2$ was only 6.78 g $CO_2$/100 g aqueous solution.

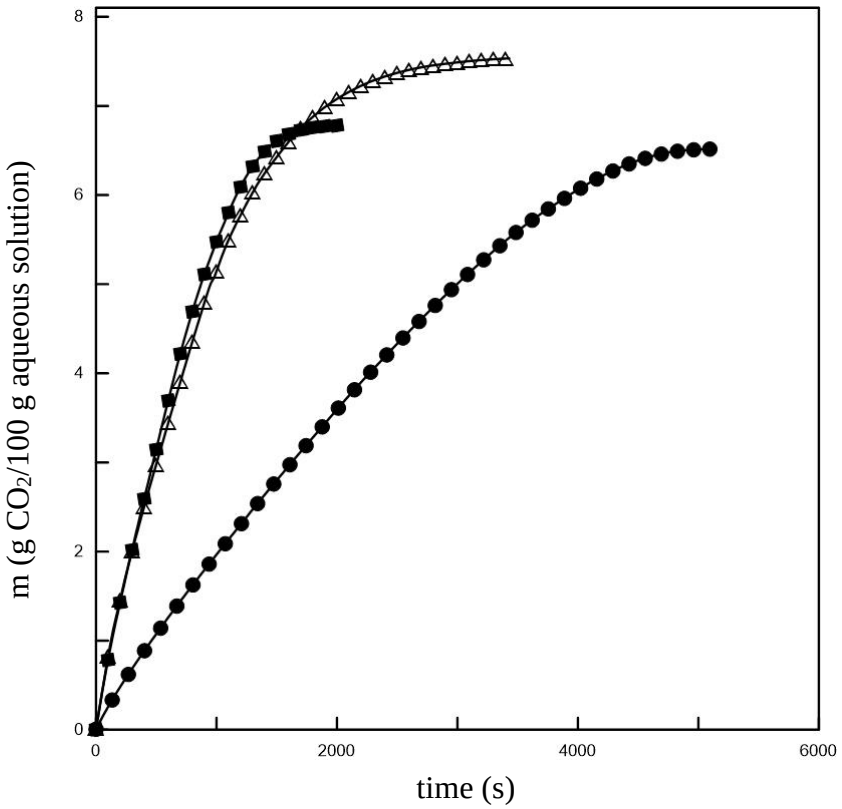


**Figure 2.** Time-dependent $CO_2$ absorption amount in $K_2CO_3$, $K_2CO_3$-[Bmim][Lys] and $K_2CO_3$-DEA aqueous solutions. $T$=313.2 K. ● $w_{K2CO3}$=0.25; △ $w_{K2CO3}/w_{[Bmim][Lys]}$=0.25/0.075; ■ $w_{K2CO3}/w_{DEA}$=0.25/0.03. Symbols: experiments from this work. Lines: trend lines.

To quantitatively demonstrate the enhancement derived from [Bmim][Lys] and DEA, we followed Chowdhury [54] and calculated the absorption rate ($V$, g $CO_2$/100 g aqueous solution/min) by the formula $0.5*m/t_{0.5}$ (m is the mass of absorbed $CO_2$, and $t_{0.5}$ is the absorption time at which 50% of the absorption capacity is achieved). The absorption rates (g $CO_2$/100 g aqueous solution/min) of $CO_2$ in aqueous solutions of $K_2CO_3$, $K_2CO_3$-[Bmim][Lys] and $K_2CO_3$-DEA were respectively 0.12, 0.34 and 0.37, indicating that DEA and [Bmim][Lys] led to very similar enhancements of the $CO_2$ absorption rate. Taking into account the much higher absorption capacity and similar absorption rate, [Bmim][Lys]-$K_2CO_3$ aqueous solution has a better application potential in the $CO_2$ capture process than DEA-$K_2CO_3$ aqueous solution.

*3.2 Corrosion behaviour*

The corrosion behaviour of carbon steel in carbonated aqueous solutions of $K_2CO_3$ and $K_2CO_3$-[Bmim][Lys] were measured. The mass fractions of $K_2CO_3$ and [Bmim][Lys] ranged from 0.15 to 0.25 and 0.025-0.075, respectively. The temperatures ranged from 303.2 K to 323.2 K.

Fig. 3 shows the effect of temperature on the potentiodynamic polarization curves of carbon steel in $CO_2$-saturated $K_2CO_3$-[Bmim][Lys] aqueous solutions. Generally, the cathodic and anodic current densities respectively refer to the metal dissolution rate and oxidant reduction rate [55]. An increase in liquid temperature tends to increase both the cathodic and anodic current densities, which may result in

an increase in both the metal dissolution rate and oxidant reduction rate, and the corrosion process can consequently be accelerated [56].

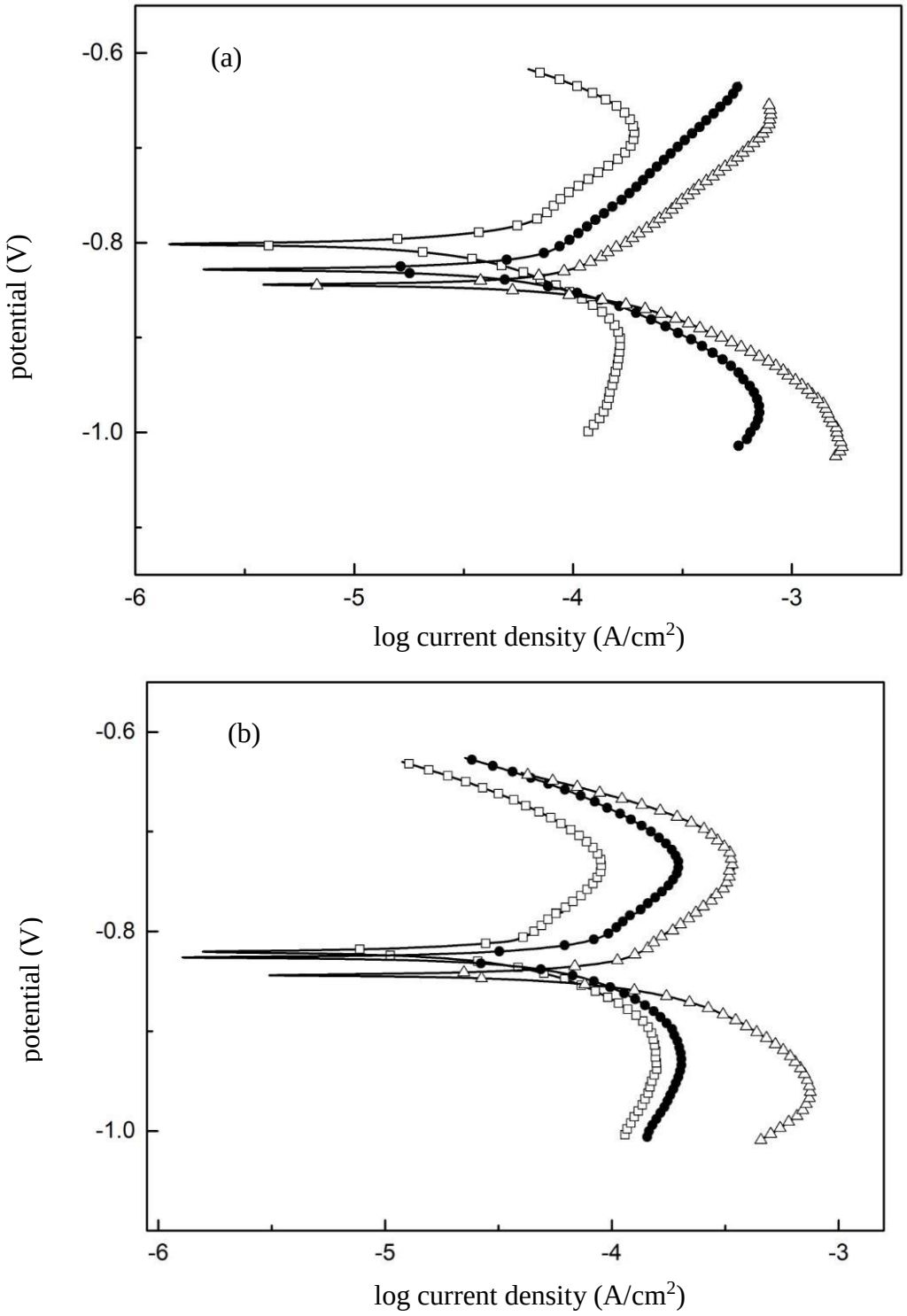


**Figure 3.** Effect of temperature on the potentiodynamic polarization curves of carbon steel in $CO_2$-saturated aqueous solutions of $K_2CO_3$-[Bmim][Lys]. $w_{[Bmim][Lys]}$=0.075. □$T$=303.2 K; ● $T$=313.2 K; △$T$=323.2 K. (a): $w_{K2CO3}$=0.15. (b): $w_{K2CO3}$=0.25. Symbols: experiments from this work. Lines: trend lines.

Fig. 4 shows the effect of solution concentration on the potentiodynamic polarization curves of carbon steel in $CO_2$-saturated aqueous solutions of $K_2CO_3$-[Bmim][Lys] and $K_2CO_3$.

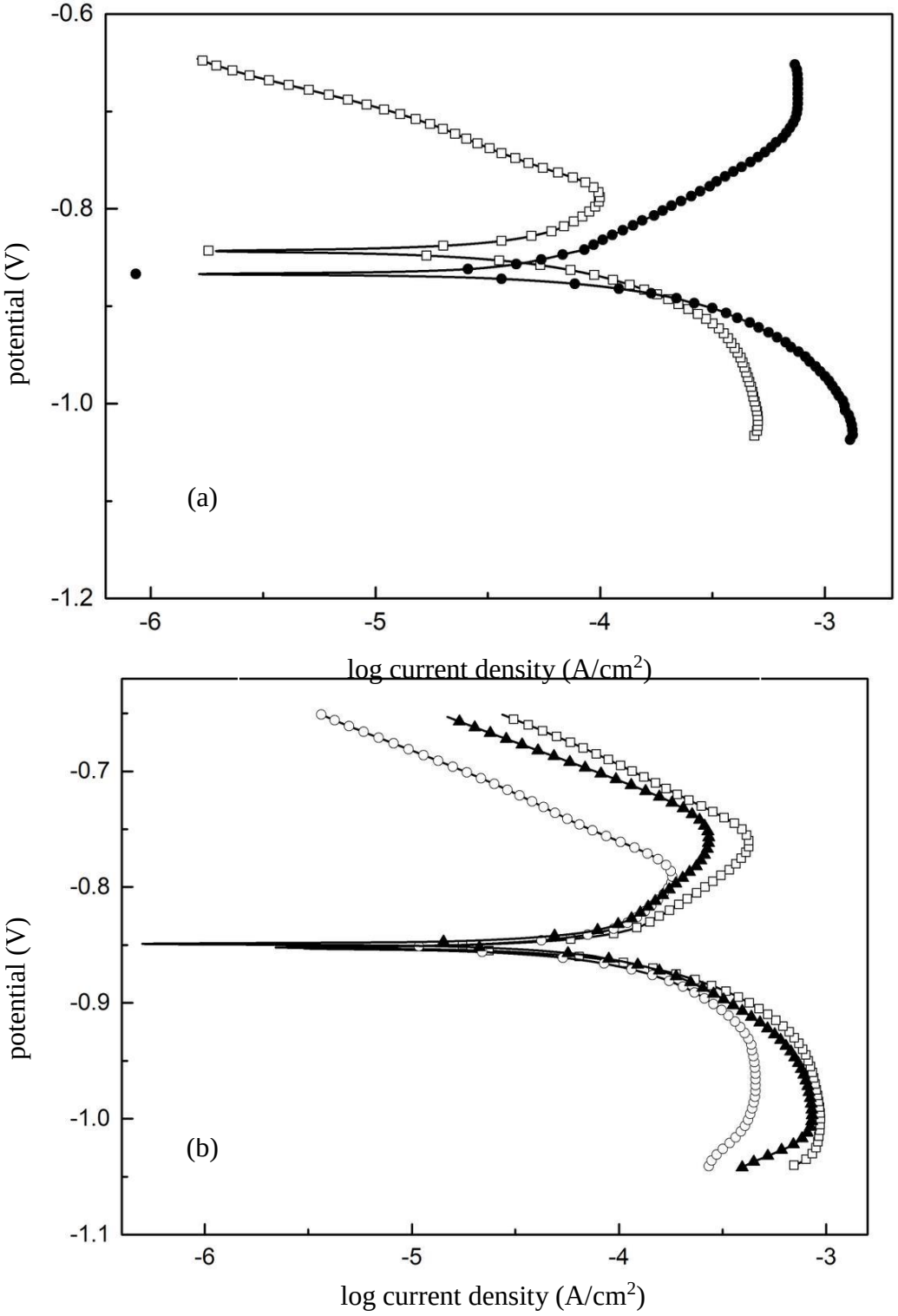


**Figure 4.** Potentiodynamic polarization curves of carbon steel in $CO_2$-saturated aqueous solutions of $K_2CO_3$-[Bmim][Lys] and $K_2CO_3$. $T$=323.2 K. (a): □ $w_{K2CO3}/w_{[Bmim][Lys]}$=0.15/0.025; ● $w_{K2CO3}$=0.175. (b): ○ $w_{K2CO3}/w_{[Bmim][Lys]}$=0.20/0.025; ▲ $w_{K2CO3}/w_{[Bmim][Lys]}$=0.20/0.05; □ $w_{K2CO3}/w_{[Bmim][Lys]}$=0.20/0.075. Symbols: experiments from this work. Lines: trend lines.

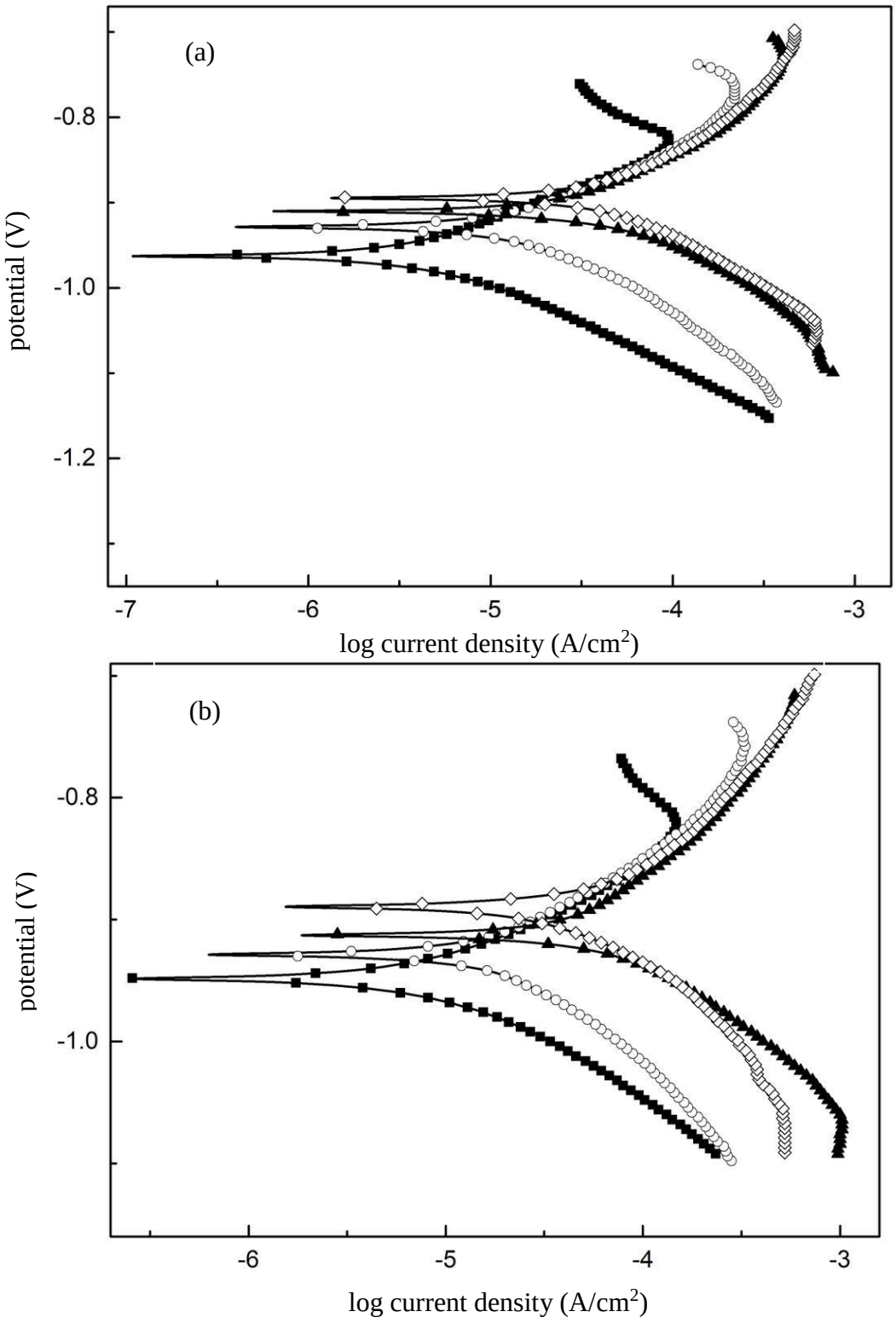


**Figure 5.** Effect of $CO_2$ loading on the potentiodynamic polarization curves of carbon steel in carbonated $K_2CO_3$-[Bmim][Lys] aqueous solutions. $w_{[Bmim][Lys]}$=0.075, $T$=313.2 K. ■α=0.1; ○α=0.2; ▲α=0.3; ◇α=0.4. (a): $w_{K2CO3}$=0.15. (b): $w_{K2CO3}$=0.20. Symbols: experiments from this work. Lines: trend lines.

One may find from Fig. 4 (a) that under the same solution concentration, the current density of carbon steel in $CO_2$-saturated $K_2CO_3$ aqueous solution was much larger than that in $CO_2$-saturated

$K_2CO_3$-[Bmim][Lys] aqueous solution, indicating the corrosion of carbon steel in $CO_2$-saturated $K_2CO_3$ aqueous solution would be more intense than that in $CO_2$-saturated $K_2CO_3$-[Bmim][Lys] aqueous solution [57-59]. Moreover, in Fig. 4 (b), with an increase in solution concentration, both the cathodic and anodic current densities increased; e.g., in the case of E/V=-0.80, the anodic current density corresponding to $w_{[Bmim][Lys]}/w_{K2CO3}$=0.025/0.20 and $w_{[Bmim][Lys]}/w_{K2CO3}$=0.075/0.20 at 323.2 K is respectively $3.16 \times 10^{-4}$ and $3.98 \times 10^{-4}$ (A/cm$^2$).

Fig. 5 shows the effect of $CO_2$ loading on the potentiodynamic polarization curves of carbon steel in carbonated $K_2CO_3$-[Bmim][Lys] aqueous solutions. One finds from the polarization curves that a change in $CO_2$ loading has a great influence on the current density of the cathode but a small effect on the anodic current density, indicating that the increase in $CO_2$ loading mainly increases the rate of oxidant reduction and thus leads to a more corrosive environment [55].

Table 2 shows the corrosion parameters obtained from the polarization curves shown in Fig. 3-5, including the corrosion potential ($E_{corr}$), the corrosion current density ($i_{corr}$) and the anodic and cathodic Tafel slopes ($\beta_a$ and $\beta_c$, respectively).

**Table 2.** Corrosion parameters obtained from the polarization curves shown in Fig. 3-5.

| Experimental categories | | | | Corrosion parameters | | | |
|---|---|---|---|---|---|---|---|
| $w_{K2CO3}$ | $w_{[Bmim][Lys]}$ | *T/K* | α | $E_{corr}$ (V) | $i_{corr}$ (A/cm$^2$) | $\beta_a$ (mV/decade) | $\beta_c$ (mV/decade) |
| 0.150 | 0.075 | 303.2 | saturated | -0.801 | 2.291E-05 | 93 | 84 |
| 0.150 | 0.075 | 313.2 | saturated | -0.828 | 3.513E-05 | 168 | 86 |
| 0.150 | 0.075 | 323.2 | saturated | -0.844 | 5.346E-05 | 152 | 94 |
| 0.250 | 0.075 | 303.2 | saturated | -0.820 | 3.076E-05 | 159 | 87 |
| 0.250 | 0.075 | 313.2 | saturated | -0.826 | 4.778E-05 | 161 | 129 |
| 0.250 | 0.075 | 323.2 | saturated | -0.844 | 7.222E-05 | 155 | 73 |
| 0.150 | 0.025 | 323.2 | saturated | -0.843 | 4.386E-05 | 105 | 57 |
| 0.175 | 0.000 | 323.2 | saturated | -0.867 | 5.957E-05 | 112 | 55 |
| 0.200 | 0.025 | 323.2 | saturated | -0.849 | 5.455E-05 | 108 | 63 |
| 0.200 | 0.050 | 323.2 | saturated | -0.852 | 5.804E-05 | 155 | 107 |
| 0.200 | 0.075 | 323.2 | saturated | -0.853 | 6.218E-05 | 92 | 67 |
| 0.150 | 0.075 | 313.2 | 0.1 | -0.963 | 1.309E-06 | 82 | 62 |
| 0.150 | 0.075 | 313.2 | 0.2 | -0.929 | 5.455E-06 | 88 | 89 |
| 0.150 | 0.075 | 313.2 | 0.3 | -0.910 | 1.069E-05 | 82 | 51 |
| 0.150 | 0.075 | 313.2 | 0.4 | -0.895 | 1.353E-05 | 112 | 94 |
| 0.200 | 0.075 | 313.2 | 0.1 | -0.949 | 3.055E-06 | 62 | 57 |
| 0.200 | 0.075 | 313.2 | 0.2 | -0.929 | 9.164E-06 | 87 | 90 |
| 0.200 | 0.075 | 313.2 | 0.3 | -0.913 | 1.549E-05 | 108 | 79 |
| 0.200 | 0.075 | 313.2 | 0.4 | -0.889 | 1.833E-05 | 91 | 99 |

In general, the reaction of [Bmim][Lys] with $CO_2$ is believed to be similar to that of alkanolamines and can be briefly described as follows [55,60,61]:

$$CO_2 + 2RNH_2 \leftrightarrow RNHCOO^- + RNH_3^+ \quad (1)$$

$$CO_2 + H_2O \leftrightarrow HCO_3^- + H^+ \quad (2)$$

$$RNHCOO^- + H_2O + H^+ \leftrightarrow RNH_3^+ + HCO_3^- \quad (3)$$

$$HCO_3^- \leftrightarrow CO_3^{2-} + H^+ \quad (4)$$

The overall reaction of $CO_2$ in $K_2CO_3$ aqueous solutions can be written as [62]:

$$CO_2 + H_2O + CO_3^{2-} \leftrightarrow 2HCO_3^- \quad (5)$$

The dissolved $CO_2$ in aqueous solutions of both [Bmim][Lys]-$K_2CO_3$ and $K_2CO_3$ was transformed into carbon species such as $HCO_3^-$ and $CO_3^{2}$, and $HCO_3^-$ is considered as a primary corroding agent. The corrosion reaction between $HCO_3^-$ and iron can be described as [55]:

$$Fe + HCO_3^- \rightarrow FeCO_3 + H^+ + 2e^- \quad (6)$$

One finds from Eqs. (1)-(6) that the $HCO_3^-$ concentration and pH are directly related to the $CO_2$ loading, $w_{[Bmim][Lys]}$ and $w_{K2CO3}$. To quantitatively show the relationship among solution concentration, $CO_2$ loading and hydrogen ion concentration ($H^+$), the pH of carbonated $K_2CO_3$-[Bmim][Lys] aqueous solution was measured at 303.2 K, as shown in Fig. 6. One may find from Fig. 6 (a) that with increasing $w_{[Bmim][Lys]}$ and $w_{K2CO3}$, the pH decreases rapidly. Moreover, the higher is the $CO_2$ loading is, the lower the pH, as also shown in the inset plot of Fig. 6 (b).

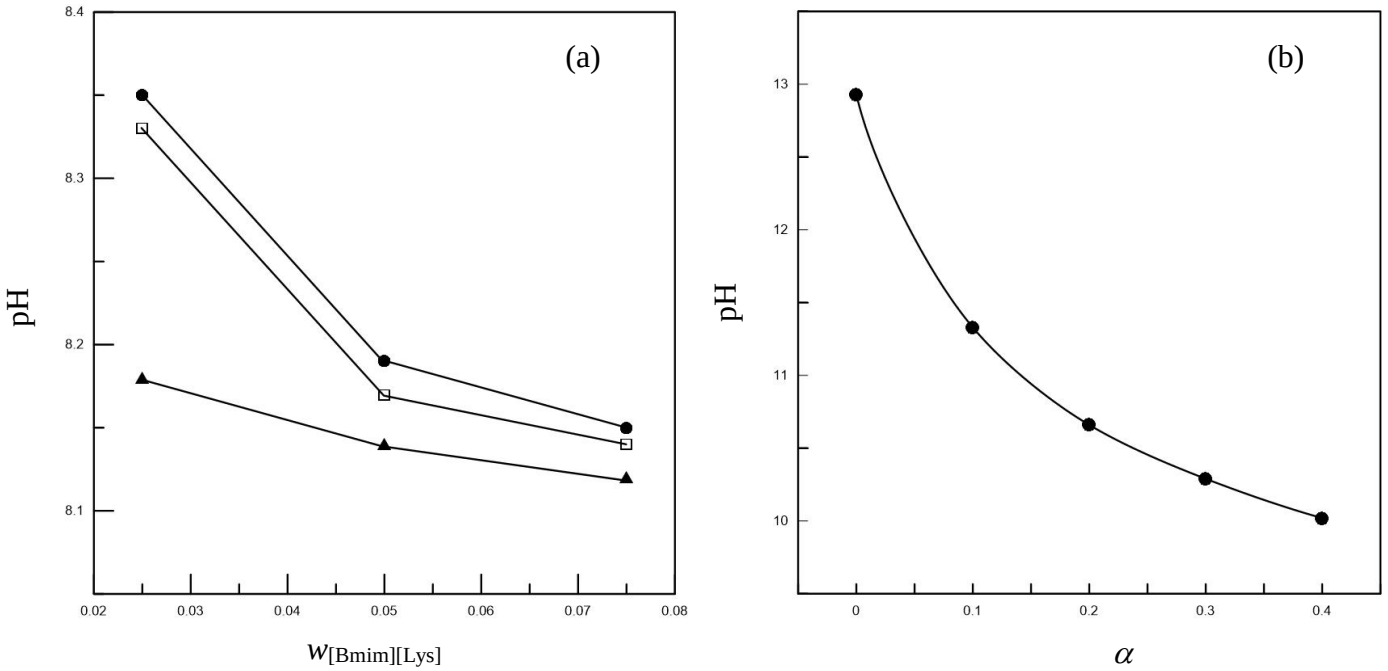


**Figure 6.** (a) Effect of [Bmim][Lys] mass fraction on the pH of $CO_2$-$K_2CO_3$-[Bmim][Lys] aqueous solutions. $CO_2$-saturated, ●$w_{K2CO3}$=0.15; □$w_{K2CO3}$=0.20; ▲$w_{K2CO3}$=0.25. (b) Effects of $CO_2$ loading on the pH of $CO_2$-$K_2CO_3$-[Bmim][Lys] aqueous solutions. ● $w_{K2CO3}/w_{[Bmim][Lys]}$=0.25/0.075. (a) and (b): $T$=303.2 K. Symbols: experiments from this work. Lines: trend lines.

It seems that the corrosion of carbon steel is dependent on many operating conditions, including the [Bmim][Lys] concentration, $K_2CO_3$ concentration, temperature and $CO_2$ loading ($HCO_3^-$). To quantitatively estimate the effects of these conditions, we calculated the corrosion rate (R) by using the following formula [63,64]:

$$R\ [mm/y] = 3.27 \times 10^{-3} \times \frac{A}{n\rho} i_{corr} \quad (7)$$

where A is the metal atomic weight, and $n$ and $\rho$ are respectively the number of transferred electrons and metal density. By combining the measured corrosion current densities and Eq. (7), the corrosion rates of carbon steel in carbonated $K_2CO_3$ aqueous solutions and carbonated $K_2CO_3$-[Bmim][Lys] aqueous solutions were determined and are presented in Tables 3-5.

**Table 3.** Corrosion rates ($R$) of carbon steel in $CO_2$-saturated $K_2CO_3$ aqueous solutions under different mass fractions of $K_2CO_3$ ($w_{K2CO3}$) and temperatures. Pressure ($p$) =101 kPa. [a]

| $w_{K2CO3}$ | $R$/(mpy) | | |
|---|---|---|---|
| | 303.2 K | 313.2 K | 323.2 K |
| 0.150 | 10.9 | 16.6 | 25.1 |
| 0.175 | 11.6 | 17.6 | 27.3 |
| 0.200 | 12.6 | 19.4 | 29.7 |
| 0.225 | 13.5 | 21.2 | 32.4 |
| 0.250 | 14.8 | 22.6 | 34.7 |

[a] Standard uncertainties $u$ are $u(T)$=0.1 K; $u(w_{K2CO3})$=±0.005; $u(p)$=2 kPa; $u(R)$=0.1 mpy.

**Table 4.** Corrosion rates ($R$) of carbon steel in $CO_2$-saturated $K_2CO_3$-[Bmim][Lys] aqueous solutions under different mass fractions of $K_2CO_3$ ($w_{K2CO3}$) and [Bmim][Lys] ($w_{[Bmim][Lys]}$) and temperatures. Pressure ($p$) =101 kPa. [a]

| $w_{K2CO3}$ | $w_{[Bmim][Lys]}$ | $R$/(mpy) | | |
|---|---|---|---|---|
| | | 303.2 K | 313.2 K | 323.2 K |
| 0.150 | 0.025 | 8.7 | 13.4 | 20.1 |
| | 0.050 | 9.5 | 14.6 | 22.4 |
| | 0.075 | 10.5 | 16.1 | 24.5 |
| 0.200 | 0.025 | 10.8 | 16.5 | 25 |
| | 0.050 | 11.4 | 17.6 | 26.6 |
| | 0.075 | 12.2 | 18.8 | 28.5 |
| 0.250 | 0.025 | 12.7 | 19.4 | 29.3 |
| | 0.050 | 13.4 | 20.4 | 30.8 |
| | 0.075 | 14.1 | 21.9 | 33.1 |

[a] Standard uncertainties $u$ are $u(T)$=0.1 K; $u(w_{K2CO3})$=±0.005; $u(w_{[Bmim][Lys]})$=±0.005; $u(p)$=2 kPa; $u(R)$=0.1 mpy.

Fig. 7 shows the effects of $w_{[Bmim][Lys]}$ (plot (a)) and $w_{K2CO3}$ (plot (b)) on the corrosion rates of carbon steel in $CO_2$-saturated $K_2CO_3$ and $CO_2$-saturated $K_2CO_3$-[Bmim][Lys] aqueous solutions. One may find that the corrosion rate increases monotonously with increasing $w_{[Bmim][Lys]}$ and $w_{K2CO3}$ at a given temperature. The amount of $HCO_3^-$ and $RNH_3^+$ tends to increase with increases in both $w_{[Bmim][Lys]}$ and $w_{K2CO3}$, as described in Eqs. (1) - (5), thus leading to an increased corrosion rate [56,65]. One may also find that when activated by [Bmim][Lys], the carbonated [Bmim][Lys]-$K_2CO_3$ aqueous solution has a lower corrosion rate at given $w_{K2CO3}$, as shown in Table 3 and Table 4. The above phenomenon may be explained by the competitive influence between the lone electron pairs in nitrogen atoms in the structure of [Bmim][Lys] molecules and the $HCO_3^-$/$RNH_3^+$ concentration in the carbonated aqueous solution. On

one hand, [Bmim][Lys] contains imidazole, and the lone electron pairs in nitrogen atoms tend to facilitate the adsorption of compounds on metallic surfaces, which may weaken the corrosion tendency [32-34,66,67].

**Table 5.** Corrosion rates ($R$) of carbon steel in $K_2CO_3$-[Bmim][Lys] aqueous solutions under different mass fractions of $K_2CO_3$ ($w_{K2CO3}$) and [Bmim][Lys] ($w_{[Bmim][Lys]}$) and $CO_2$ loadings. T=313.2 K. Pressure ($p$) =101 kPa. [a]

| $w_{K2CO3}$ | $w_{[Bmim][Lys]}$ | $R$/(mpy) | | | |
|---|---|---|---|---|---|
| | | α=0.1 | α=0.2 | α=0.3 | α=0.4 |
| 0.150 | 0.025 | 2.3 | 4.7 | 7.0 | 8.3 |
| | 0.050 | 1.4 | 3.6 | 5.8 | 7.4 |
| | 0.075 | 0.6 | 2.5 | 4.9 | 6.2 |
| 0.200 | 0.025 | 3.3 | 6.4 | 9.7 | 11.0 |
| | 0.050 | 1.9 | 5.2 | 8.4 | 9.8 |
| | 0.075 | 1.4 | 4.2 | 7.1 | 8.4 |
| 0.250 | 0.025 | 4.3 | 8.7 | 13.7 | 15.6 |
| | 0.050 | 3.1 | 7.3 | 12.1 | 14.2 |
| | 0.075 | 1.9 | 6.6 | 10.5 | 12.5 |

[a] Standard uncertainties $u$ are $u(T)$=0.1 K; $u(w_{K2CO3})$=±0.005; $u(w_{[Bmim][Lys]})$=±0.005; $u(p)$=2 kPa; $u(R)$=0.1 mpy.

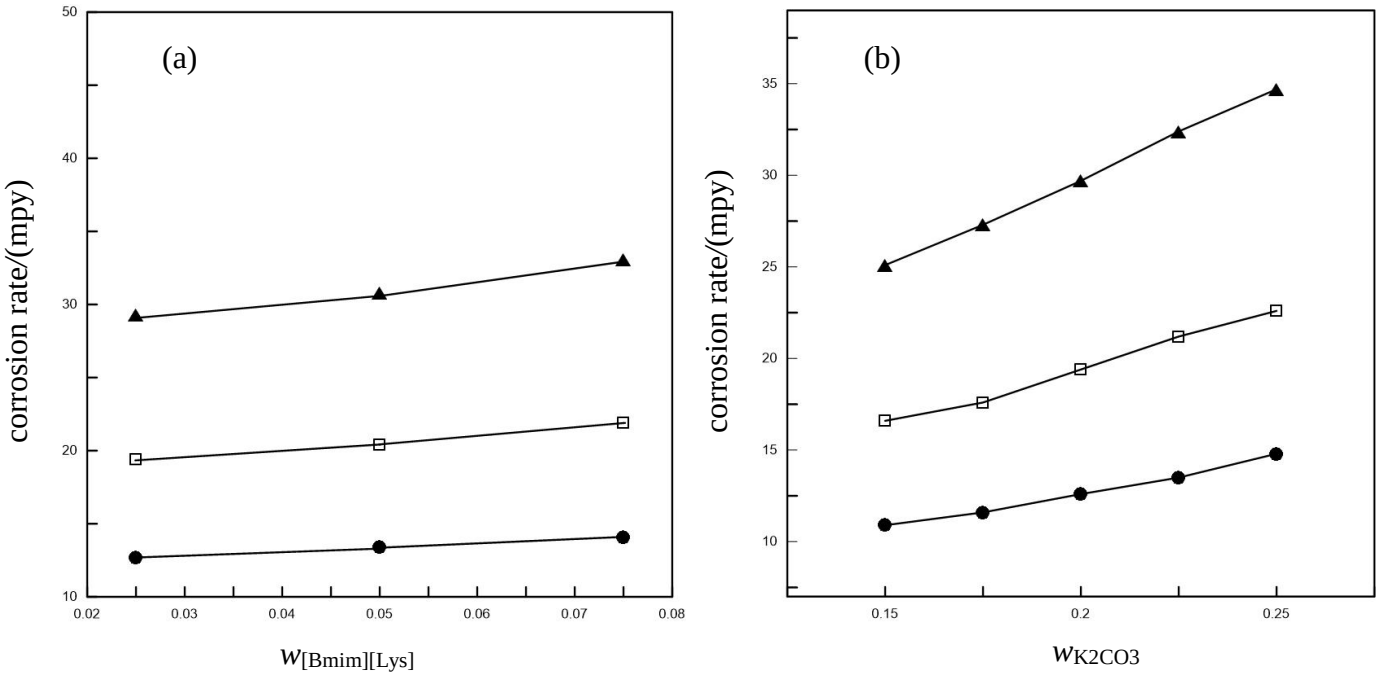


**Figure 7.** (a) Effect of mass fraction of [Bmim][Lys] on the corrosion rate of carbon steel in $CO_2$-saturated $K_2CO_3$-[Bmim][Lys] aqueous solutions. $w_{K2CO3}$=0.25. (b) Effect of mass fraction of $K_2CO_3$ on the corrosion rate of carbon steel in $CO_2$-saturated $K_2CO_3$ aqueous solutions. $w_{[Bmim][Lys]}$=0.0. (a) and (b): ●T=303.2 K; □T=313.2 K; ▲T=323.2 K. Symbols: experiments from this work. Lines: trend lines.

On the other hand, increasing the concentration of [Bmim][Lys] in the carbonated $K_2CO_3$-[Bmim][Lys] aqueous solution may also lead to an increase in the concentration of $HCO_3^-$/$RNH_3^+$, thus increasing the corrosion rate, as shown in Table 4. Taking into account such competitive influences, $w_{[Bmim][Lys]}$ is no greater than 0.075 in this work, i.e., the corrosion rate obviously decreased only when a small amount of [Bmim][Lys] was added into $K_2CO_3$ aqueous solution.

Fig. 8 shows the effects of $CO_2$ loading on the corrosion rate of carbon steel in carbonated $K_2CO_3$-[Bmim][Lys] aqueous solutions and indicates that the corrosion rate increases with increasing $CO_2$ loading. In general, increasing the $CO_2$ loading results in higher amounts of $HCO_3^-$ and $RNH_3^+$, which in turn dissociate and eventually produce more hydrogen ion ($H^+$) [55,56,68]. The increase in the $H^+$ amount due to increased $CO_2$ loading is confirmed by the pH reduction reported in Fig. 6 (b). The increase in the amounts of $H^+$ and $HCO_3^-$ causes the corrosion process to proceed faster, thus resulting in a higher corrosion rate. Frolova [65] studied the effect of $HCO_3^-$ concentration on corrosion rate of low- and high-strength steel in 1 N sodium carbonate solution. Their results showed that the corrosion rate increased with increasing $HCO_3^-$. Moreover, at a given $CO_2$ loading and $w_{K2CO3}$, the corrosion rate decreased with increasing $w_{[Bmim][Lys]}$ due to the competitive influence between the lone electron pairs in nitrogen atoms in the structure of [Bmim][Lys] molecules and the $HCO_3^-$ concentration in the carbonated aqueous solution, as addressed previously.

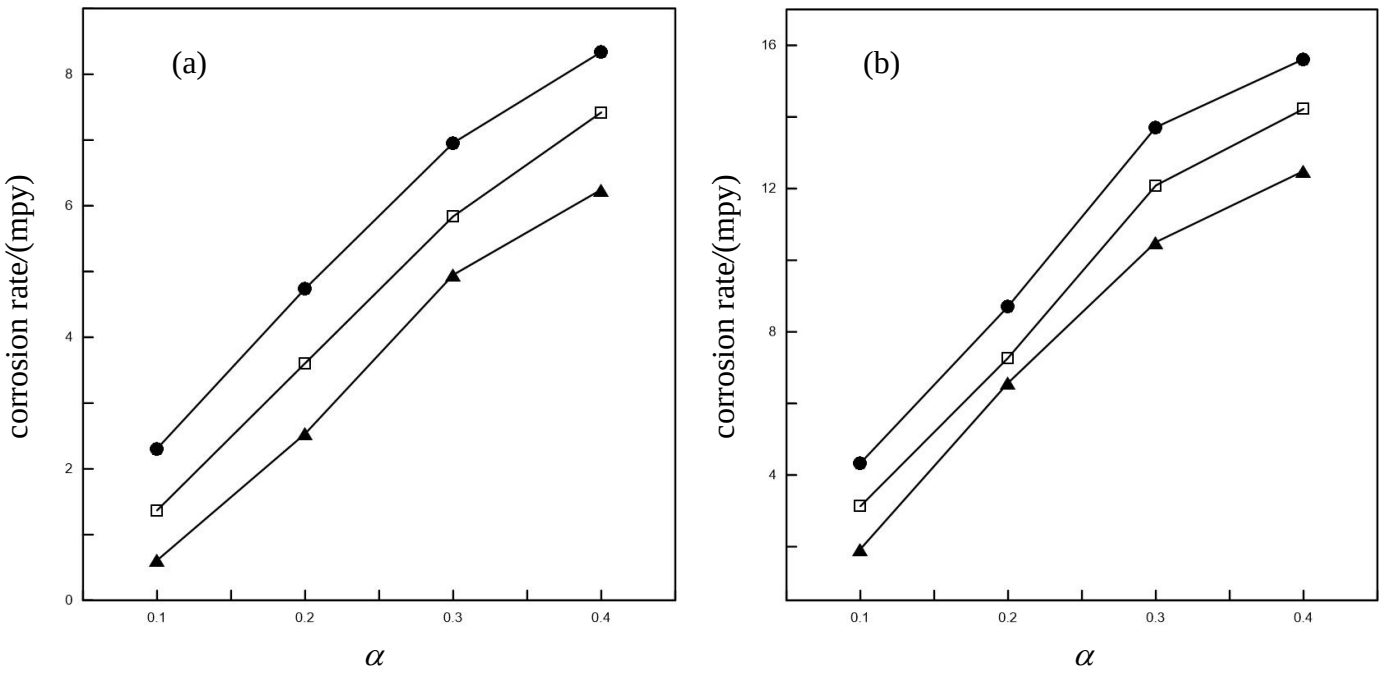


**Figure 8.** Effect of $CO_2$ loading on the corrosion rate of carbon steel in carbonated $K_2CO_3$-[Bmim][Lys] solution. T=313.2 K. ● $w_{[Bmim][Lys]}$= 0.025; □$w_{[Bmim][Lys]}$=0.05; ▲ $w_{[Bmim][Lys]}$= 0.075. (a): $w_{K2CO3}$=0.15. (b): $w_{K2CO3}$=0.25. Symbols: experiments from this work. Lines: trend lines.

In addition to the corrosion rate of carbon steel in carbonated $K_2CO_3$ aqueous solution and carbonated $K_2CO_3$-[Bmim][Lys] aqueous solution, the corrosion rate of carbon steel in $CO_2$-saturated $K_2CO_3$ (25%)-DEA (3%) aqueous solution was also measured at 313.3 K in this work. The obtained

result was 22.1 mpy, which is higher than the corrosion rate of carbon steel in $CO_2$-saturated $K_2CO_3$ (25%)-[Bmim][Lys] (7.5%) (21.9 mpy), indicating that [Bmim][Lys] has a lower corrosion tendency toward carbon steel than DEA and thus has better application potential in the $CO_2$ capture process.

## 4. CONCLUSIONS

In this work, the $CO_2$ capture process and corrosion of carbon steel in [Bmim][Lys]-$K_2CO_3$ aqueous solutions were investigated. The effects of temperature, solution concentration and $CO_2$ loading on the corrosion rate were demonstrated. Our results show that the following:

(1) At a given $w_{K2CO3}$ and $w_{[Bmim][Lys]}$, the corrosion rate of carbon steel in $CO_2$-saturated $K_2CO_3$-[Bmim][Lys] aqueous solution increases with increasing temperature. At a given $w_{K2CO3}$, $w_{[Bmim][Lys]}$ and temperature, the corrosion rate obviously increases with increasing $CO_2$ loading;

(2) Increases in both $w_{K2CO3}$ and $w_{[Bmim][Lys]}$ tend to decrease the pH of $CO_2$-saturated $K_2CO_3$-[Bmim][Lys] aqueous solution, thus increasing the $H^+$ concentration and the corrosion rate of carbon steel;

(3) There may exist a competitive influence between the lone electron pairs in nitrogen atoms and the $HCO_3^-$ concentration; the corrosion rate of carbon steel obviously decreased only when a small amount of [Bmim][Lys] was added to $K_2CO_3$ aqueous solution;

(4) The [Bmim][Lys]-activated $K_2CO_3$ aqueous solution had a higher $CO_2$ absorption capacity, higher $CO_2$ absorption rate and lower corrosion rate of carbon steel than $K_2CO_3$ aqueous solution at a given $K_2CO_3$ mass fraction;

(5) Compared with the commercially applied DEA (3%)-$K_2CO_3$ (25%) aqueous solution, the [Bmim][Lys] (7.5%)-activated $K_2CO_3$ (25%) aqueous solution produced a similar $CO_2$ absorption rate; however, the latter solution has the advantages of a higher $CO_2$ absorption capacity, lower corrosion of carbon steel, higher concentration and lower water content, and thus has better application potential in the $CO_2$ capture process.

ACKNOWLEDGMENTS
The authors appreciate the financial support from the National Natural Science Foundation of China (No. 51776072) and the Fundamental Research Funds for the Central Universities (No. 2017XS132 and No. 2018MS116).

## References

1. A. Višković, V. Franki, V. Valentić, *Energy*, 70 (2014) 325.
2. H.R. Stuart, *Science*, 325 (2009) 1647.
3. P.C. Tseng, W.S. Ho, D.W. Savage, *AlChE J.*, 34 (1988) 922.
4. Y. Maham, A.E. Mather, C. Mathonat, *J. Chem. Thermodyn.*, 32 (2000) 229.
5. C. Zheng, D. Liu, Q. Yang, C. Zhong, J. Mi, *Ind. Eng. Chem. Res.*, 48 (2009) 10479.
6. S.P. Yan, M.X. Fang, W.F. Zhang, S.Y. Wang, Z.K. Xu, Z.Y. Luo, K.F. Cen, *Fuel Process. Technol.*, 88 (2007) 501.
7. X.S. Li, H.J. Wu, Y.G. Li, Z.P. Feng, L.G. Tang, S.S. Fan, *J. Chem. Thermodyn.*, 39 (2007) 417.

8. F. Barzagli, F. Mani, M. Peruzzini, *Energy Environ. Sci.,* 3 (2010) 772.
9. G. Bińczak, W. Moniuk, Z. Mordecka, C. Możeński, *Chem. Process Eng.*, 37 (2016) 83.
10. K.A. Mumford, K.H. Smith, C.J. Anderson, S. Shen, W. Tao, Y.A. Suryaputradinata, A. Qader, B. Hooper, R.A. Innocenzi, S.E. Kentish, G.W. Stevens, *Energy Fuels*, 26 (2012) 138.
11. V. Augugliaro, L. Rizzuti, *Chem. Eng. Sci.,* 42 (1987) 2339.
12. G. Hu, N.J. Nicholas, K.H. Smith, K.A. Mumford, S.E. Kentish, G.W. Stevens, *Int. J. Greenhouse Gas Control*, 53 (2016) 28.
13. S. Zhang, Y. Lu, *Chem. Eng. J.,* 279 (2015) 335.
14. H. Thee, K.H. Smith, G.D. Silva, S.E. Kentish, G.W. Stevens, *Chem. Eng. J.*, 181–182 (2012) 694.
15. S. Shen, Y. Yang, S. Ren, *Fluid Phase Equilib.*, 367 (2014) 38.
16. S. Masoumi, P. Keshavarz, S. Ayatollahi, M. Mehdipour, Z. Rastgoo, *Energy Fuels,* 27 (2013) 5423.
17. J.T. Cullinane, B.A. Oyenekan, J. Lu, G.T. Rochelle, Aqueous piperazine/potassium carbonate for enhanced $CO_2$ capture, in: *Greenhouse Gas Control Technologies 7*, Elsevier Science Ltd, (2005) Oxford, United Kingdom.
18. J.M. Plaza, E. Chen, G.T. Rochelle, *AIChE J.*, 56 (2010) 905.
19. H. Thee, Y.A. Suryaputradinata, K.A. Mumford, K.H. Smith, G.d. Silva, S.E. Kentish, G.W. Stevens, *Chem. Eng. J.*, 210 (2012) 271.
20. T.N.G. Borhani, V. Akbari, M. Afkhamipour, M.K.A. Hamid, Z.A. Manan, *Chem. Eng. Sci.,* 122 (2015) 291.
21. T.N.G. Borhani, V. Akbari, M.K.A. Hamid, Z.A. Manan, *J. Ind. Eng. Chem.,* 22 (2015) 306.
22. M.S. Shaikh, M.S. Azmi, M.A. Bustam, G. Murshid, *Appl. Mech. Mater.*, 625 (2014) 19.
23. H. Thee, N.J. Nicholas, K.H. Smith, G. da Silva, S.E. Kentish, G.W. Stevens, *Int. J. Greenhouse Gas Control*, 20 (2014) 212.
24. G. Hu, K.H. Smith, Y. Wu, S.E. Kentish, G.W. Stevens, *Energy Fuels*, 31 (2017) 4280.
25. Y. Li, L.a. Wang, Z. Zhang, X. Hu, Y. Cheng, C. Zhong, *Energy Fuels*, 32 (2018) 3637.
26. S. Paul, K. Thomsen, Int. *J. Greenhouse Gas Control*, 8 (2012) 169.
27. D. Wappel, G. Gronald, R. Kalb, J. Draxler, *Int. J. Greenhouse Gas Control*, 4 (2010) 486.
28. L.M. Galan Sanchez, G.W. Meindersma, A.B. de Haan, *Chem. Eng. J.*, 166 (2011) 1104.
29. Y.S. Zhao, X.P. Zhang, Y.P. Zhen, H.F. Dong, G.Y. Zhao, S.J. Zeng, X. Tian, S.J.Zhang, *Int. J. Greenhouse Gas Control*, 5 (2011) 367.
30. H. Hu, F. Li, Q. Xia, X.D. Li, L. Liao, M.H. Fan, *Int. J. Greenhouse Gas Control*, 31 (2014) 33.
31. D. Wappel, G. Gronald, R. Kalb, J. Draxler, *Int. J. Greenhouse Gas Control,* 4 (2010) 486.
32. R. Gašparac, C.R. Martin, E. Stupnišek‐Lisac, *J. Electrochem. Soc.,* 147 (2000) 548.
33. K.M. Manamela, L.C. Murulana, M.M. Kabanda, E.E. Ebenso, *Int. J. Electrochem. Sci.,* 9 (2014) 3029.
34. M.A. Quraishi, M.Z.A. Rafiquee, S. Khan, N. Saxena, *J. Appl. Electrochem.* 37 (2007) 1153.
35. Q.B. Zhang, Y.X. Hua, *Electrochim. Acta,* 54 (2009) 1881.
36. Q.B. Zhang, Y.X. Hua, *Mater. Chem. Phys.,* 119 (2010) 57.
37. H. Ashassi-Sorkhabi, M. Es'Haghi, *Mater. Chem. Phys.*, 114 (2009) 267.
38. X. Zheng, S. Zhang, W. Li, M. Gong, L. Yin, *Corros. Sci.*, 95 (2015) 168.
39. P. Sharma, S.D. Park, I.H. Baek, K.T. Park, Y. Yoon, II, S.K. Jeong, *Fuel Process. Technol.*, 100 (2012) 55.
40. B. Lv, G. Jing, Y. Qian, Z. Zhou, *Chem. Eng. J.*, 289 (2016) 212.
41. B.E. Gurkan, J.C. Fuente, De La, E.M. Mindrup, L.E. Ficke, B.F. Goodrich, E.A. Price, W.F. Schneider, J.F. Brennecke, *J. Am. Chem. Soc.*, 132 (2010) 2116.
42. D. Fu, P. Zhang, L. Wang, *Energy*, 113 (2016) 1.
43. P. Zhang, X.F. Tian, D. Fu, *Energy*, 161 (2018) 1122.
44. D. Fu, P. Zhang, C. Mi, *Energy*, 101 (2016) 288.
45. Z.M. Zhou, G.H. Jing, L.J Zhou, *Chem. Eng. J.*, 204–206 (2012) 235.

46. Y. Gao, F. Zhang, K. Huang, J.W. Ma, Y.T. Wu, Z.B. Zhang, *Int. J. Greenhouse Gas Control,* 19 (2013) 379.
47. H. Yu, Y.T. Wu, Y.Y. Jiang, Z. Zhou, Z.B. Zhang, *New J. Chem.*, 33 (2009) 2385.
48. Y. Cao, T. Mu, *Ind. Eng. Chem. Res.*, 53 (2014) 8651.
49. S. Mazinani, R. Ramazani, A. Samsami, A. Jahanmiri, B. Van der Bruggen, S. Darvishmanesh, *Fluid Phase Equilib.*, 396 (2015) 28.
50. R.H. Weiland, J.C. Dingman, D.B. Cronin, G.J. Browning, *J. Chem. Eng. Data*, 43 (1998) 378.
51. T.G. Amundsen, L.E. Oi, D.A. Eimer, *J. Chem. Eng. Data*, 54 (2009) 3096.
52. D. Fu, H. Hao, F. Liu, *J. Mol. Liq.*, 188 (2013) 37.
53. D. Fu, J. Xie, *J. Chem. Thermodyn.*, 102 (2016) 310.
54. F.A. Chowdhury, H. Yamada, T. Higashii, K. Goto, M. Onoda, *Ind. Eng. Chem. Res.*, 52 (2013) 8323.
55. A. Veawab, P. Tontiwachwuthikul, A. Chakma, *Ind. Eng. Chem. Res.*, 38 (1999) 3917.
56. M.F. Hamada, T.M. Zewail, H.A. Farag, *Corros. Eng., Sci. Technol.*, 49 (2014) 209.
57. S. Zhang, R. Shi, Y. Chen, M. Wang, *J. Alloys Compd.*, 731 (2018) 1230.
58. S. Zhang, R. Shi, Y. Tan, *J. Alloys Compd.*, 711 (2017) 155.
59. Y.Z. Jing, S.L. Wang, Y.Y. Chen, M.G. Bao ,L. Liu, *Int. J. Electrochem.* Sci., 13 (2018) 7629.
60. Y.S. Sistla, A. Khanna, *Chem. Eng. J.*, 273 (2015) 268.
61. P.S. Kumar, J.A. Hogendoorn, G.F. Versteeg, P.H.M. Feron, *AIChE J.*, 49 (2003) 203.
62. D. Wappel, S. Joswig, A.A. Khan, K.H. Smith, S.E. Kentish, D.C. Shallcross, G.W. Stevens, *Int. J. Greenhouse Gas Control*, 5 (2011) 1454.
63. C. Yu, H.W. Wang, X.H. Gao, *Int. J. Electrochem. Sci.,* 13 (2018) 6059.
64. M.N. Ilman, Kusmono, *Case Studies in Eng. Failure Anal.*, 2 (2014) 1.
65. L.V. Frolova, M.N. Fokin, V.E. Zorina, *Prot. Met.*, 33 (1997) 249.
66. L.M. Rodríguez-Valdez, W. Villamisar, M. Casales, J.G. González-Rodriguez, A. Martínez-Villafañe, L. Martinez, D. Glossman-Mitnik, *Corros. Sci.*, 48 (2006) 4053.
67. X. Zhou, H. Yang, F. Wang, *Electrochim. Acta*, 56 (2011) 4268.
68. G.H. Sedahem, *J. Appl. Electrochem.*, 15 (1985) 777.